On the Dynamics of Adjustment in the *f*-Plane Shallow Water Adjoint System

MICHAEL C. MORGAN

Department of Atmospheric and Oceanic Sciences, University of Wisconsin–Madison, Madison, Wisconsin

(Manuscript received 4 April 2017, in final form 19 December 2017)

ABSTRACT

Analytic results and numerical experimentation reveal that a "backward" integration of the adjoint of the shallow water system linearized about a basic state at rest on an f plane is characterized by a radiation of gravity wave–like structures and the emergence of a steady adjoint state. The earlier adjoint states are linked to the prescribed adjoint state (i.e., the adjoint forcing) through the locally conserved dynamical adjoint variables of the shallow water system: the sensitivity to "balanced height" ($\hat{\eta}_b$) and the sensitivity to potential vorticity (PV) $\hat{q}$. The sensitivity to balanced height is determined by the prescribed adjoint sensitivity forcings for the flow, $\hat{u}$ and $\hat{v}$, and height (fluid depth), $\hat{\eta}$: $\hat{\eta}_b = \hat{\eta} - (g/f)(\partial\hat{v}/\partial x - \partial\hat{u}/\partial y)$. The sensitivity to PV is diagnosed from the inversion of an elliptic operator relating the sensitivity to PV to the distribution of $\hat{\eta}_b$.

The sensitivity to PV determines the long-time ($t \to \infty$), steady behavior of the adjoint sensitivity to height, $\hat{\eta}_{t\to-\infty} = -(f/H^2)\hat{q}$. In the vicinity of the initial adjoint forcing, the long-time, steady-state behavior of the adjoint system (linearized about a state at rest) is characterized by nondivergent sensitivities to the flow that resemble geostrophic balance: $\hat{u}_{t\to-\infty} = (1/H)\partial\hat{q}/\partial y$ and $\hat{v}_{t\to-\infty} = (1/H)\partial\hat{q}/\partial x$. The process by which this long-time, nondivergent, adjoint state emerges is termed *adjoint adjustment*. For the system considered, sensitivities to the ageostrophic and irrotational components of the flow vanish for the adjusted state near the prescribed adjoint forcing.

1. Introduction

a. Background

The adjoint of a numerical weather prediction (NWP) model evaluates the sensitivity of a differentiable function of the model forecast state (known as the response function) to changes in the forecast trajectory and boundary conditions at earlier times. The adjoint-derived sensitivity is defined as the gradient of the response function with respect to the model state, including the boundary conditions. Adjoints of NWP models are developed from the tangent linear model (TLM) of the corresponding NWP model linearized about a specific forecast trajectory. At the coding level, the adjoint model represents the line-by-line transpose of the coded TLM.

Adjoint-derived forecast sensitivity gradients are used in a variety of meteorological applications. For four-dimensional variational data assimilation (4DVAR), the adjoint model is used along with minimization algorithms to determine an optimal analysis of a model initial state by combining knowledge of the misfit between a model forecast trajectory and observations, as well as knowledge of the error covariances associated with each (e.g., Talagrand and Courtier 1987). In this context, the adjoint model integrates backward in time the gradient of a response function defining the weighted misfit between observations and an initial forecast trajectory. Adjoint models have been applied also to problems concerning parameter estimation and stability analysis (e.g., Hall et al. 1982). The computation of optimal perturbations, and in particular "singular vectors" (Farrell 1989; Buizza et al. 1993), requires also an adjoint model. Assuming a perfect model and some measure of forecast error, an adjoint model can be used also to evaluate possible initial condition errors (Rabier et al. 1996; Klinker et al. 1998; Langland et al. 2002). Adjoints of NWP models are used also in case studies of weather systems. In such studies, physical interpretations of the sensitivity fields, their evolution, and their relation to the basic-state model fields from which they are described are used to apprehend the impacts of perturbations to dynamical processes associated with the weather systems (e.g., Errico and Vukićević 1992; Vukićević and Raeder 1995; Keller et al. 2006; Kleist and Morgan 2005a,b; Hoover and Morgan 2011; Doyle et al. 2014; Hoover 2015).

Corresponding author: Michael C. Morgan, mcmorgan@wisc.edu

DOI: 10.1175/JAS-D-17-0100.1

b. Motivation

From these earlier synoptic case studies, an interesting, but as yet unexplained, behavior of the adjoint-derived forecast sensitivity gradients (*sensitivity gradients* for short) has been noted—short-term (i.e., less than 6 h) backward integrations of sensitivity gradients for *particular response functions* are characterized by a "gravity wave like" structure in the sensitivities to the wind components [e.g., Figs. 9 and 11 of Errico and Vukićević (1992)]. Errico and Vukicìevicì assert that the patterns seen in the sensitivities to the horizontal wind components for short-term adjoint integrations describe the sensitivity to the specification of gravity wave (wind) components at an earlier time. For longer time adjoint integrations, the sensitivity to gravity wave–like structures is significantly reduced, producing features that are more coherent in space [e.g., Figs. 7 and 13 of Errico and Vukićević (1992)]. Further, Errico and Vukićević (1992, p. 1652) suggest that for these longer-time adjoint integrations, the adjoint sensitivities imply that "the impact of geostrophic perturbations on [the response function, surface pressure at a point] is described by the combined [horizontal] velocity and height adjoint [sensitivities]."

Despite these intriguing emergent relationships between sensitivities to wind and height that are suggestive of some sort of dynamical "balance" seen in NWP adjoint model output in these and other cases, there are no published studies exploring the dynamics of the emergence of balanced adjoint states, as the adjoint state evolves backward in time. Further, there are no discussions of under what circumstances this balance might not be expected to emerge. The emergence of balanced adjoint states and the transient behavior of the sensitivity to the imbalance are the central focuses of this paper.

c. Approach and paper structure

This work explores the (backward) evolution of adjoint-derived forecast sensitivities and the emergence of a "balanced" adjoint state. Specifically, a fundamental question of adjoint sensitivity gradient evolution will be addressed, How is adjoint state information "accumulated" dynamically within and across variables as an adjoint model is integrated (backward in time)? This will be accomplished by performing a set of numerical experiments verifying analytical results (described below) that provide a solid theoretical underpinning for an adjustment process during adjoint model integrations suggested empirically in the literature referenced above.

The adjoint of a shallow water (SW) system linearized about an at-rest basic state is used to demonstrate and interpret analytically and numerically the adjustment process observed in prior studies. The analysis reveals the existence of a conserved dynamical variable that describes the long-term (balanced) adjoint state that emerges after a period of adjustment. In section 2 the shallow water system is reviewed briefly and its adjoint system is developed. The conserved dynamical variable is derived and additional diagnostics useful in interpreting the backward evolution of the sensitivity fields are also derived. In section 3 the experimental setup and results of numerical experiments affirming the results of section 2 are discussed. A discussion of these results and their significance, as well as an outline for future studies, is found in the concluding section.

2. SW forward and adjoint systems

a. SW system and geostrophic adjustment

The SW system over a flat lower boundary linearized about a basic state at rest on an f plane is given by

$$\frac{\partial u'}{\partial t} = fv' - g\frac{\partial \eta}{\partial x}, \quad \frac{\partial v'}{\partial t} = -fu' - g\frac{\partial \eta}{\partial y}, \quad \text{and}$$

$$\frac{\partial \eta}{\partial t} = -H\left(\frac{\partial u'}{\partial x} + \frac{\partial v'}{\partial y}\right), \tag{1}$$

where u' and v' represent departures of the zonal and meridional flows from rest, respectively, and h represents the perturbation fluid depth (or "height") from the at-rest depth, H. The system possesses a locally conserved, dynamical variable, the linearized shallow water potential vorticity (SWPV), $q' = (1/H)(\partial u'/\partial x) + (1/H)(\partial v'/\partial x) - (f\eta)/H^2$.

The forward SW system may be combined to form a single wave equation,

$$\frac{\partial^2 \eta}{\partial t^2} - c^2\nabla^2\eta + f^2\eta = -fH^2q'(x, y, t = 0), \tag{2}$$

where $c^2 = gH$ is the phase speed and group velocity of nonrotating shallow water gravity waves. The homogeneous solution to this equation is characterized by inertial gravity waves, while the forced, steady response height field to an initial distribution of PV is given by the distribution of η_b, the "balanced height field." The statement of PV invertibility for the shallow water system,

$$\nabla^2\eta_b - \frac{f^2}{gH}\eta_b = \frac{Hf}{g}q'(x, y, t = 0), \tag{3}$$

relates a given distribution of a SWPV q' to the geostrophically balanced height η_b through the solution of an elliptic (3). Recall that the height η and η_b differ in that the balanced height is diagnosed from first calculating the

SWPV associated with the horizontal velocity field (u' and v') and η, and then solving (3) for η_b.

From (2) it is seen that solutions to the linearized shallow water system on an f plane are characterized by a steady height field (η_b) and a geostrophically balanced wind [$\mathbf{V}_g = (g/f)\hat{\mathbf{k}} \times \nabla\eta_b$] associated with a steady distribution of PV. Superposed on this solution are unbalanced fields of height and wind associated with propagating gravity waves with zero PV.

The shallow water system provides the underpinnings of our understanding of the prevalence of (near) geostrophic balance in rotating fluids. Geostrophic (or Rossby) adjustment is the process by which a distribution of mass and wind fields that are not *locally* geostrophically balanced will tend to become balanced locally (Rossby 1938; Washington 1964; Errico 1989). Any initial geostrophic imbalance projects onto the inertial gravity waves of the system and will propagate away from the region of initial imbalance. If the imbalance is restricted to a local region, it will eventually leave behind a stationary geostrophic field of linearized potential vorticity from which a steady height field, $\eta = \eta_b$, and steady geostrophic winds, $u' = u_g = -(g/f)(\partial\eta\partial y)$ and $v' = v_g = (g/f)(\partial\eta\partial x)$, may be diagnosed.

b. *Adjoint of system*

The adjoint shallow water system[1] is given by

$$-\frac{\partial\hat{u}}{\partial t} = -f\hat{v} + H\frac{\partial\hat{\eta}}{\partial x}, \quad -\frac{\partial\hat{v}}{\partial t} = +f\hat{u} + H\frac{\partial\hat{\eta}}{\partial y}, \quad \text{and}$$
$$-\frac{\partial\hat{\eta}}{\partial t} = g\left(\frac{\partial\hat{u}}{\partial x} + \frac{\partial\hat{v}}{\partial y}\right). \tag{4}$$

It is readily shown that the system possesses a locally conserved, dynamical variable, termed (for reasons to be discussed later) the "sensitivity to balanced height,"

$$\hat{\eta}_b = \hat{\eta} - \frac{g}{f}\left(\frac{\partial\hat{v}}{\partial x} - \frac{\partial\hat{u}}{\partial y}\right). \tag{5}$$

The adjoint SW system [(4)] may be combined to form a wave equation,

$$\frac{\partial^2\hat{\eta}}{\partial t^2} - c^2\nabla^2\hat{\eta} + f^2\hat{\eta} = f^2\hat{\eta}_b(x, y, t = t_f). \tag{6}$$

The homogeneous wave solution to (6) is characterized by a dispersion relation identical to that of shallow water inertia–gravity waves, while the forced, steady response (sensitivity to height) to a final time distribution of the sensitivity is given by the distribution of $\hat{\eta}_b$.

It is worth noting that, with the exception of an exchange of variables, g and H, systems (1) and (4) are algebraically identical and are self-adjoint as the wave equations derived from systems (2) and (6).

The adjoint to the shallow water PV inversion [(3)] is

$$\nabla^2\hat{q} - \frac{f^2}{gH}\hat{q} = \frac{Hf}{g}\hat{\eta}_b(x, y, t = t_f). \tag{7}$$

The sensitivity to shallow water PV $\hat{q}$ is therefore (within a fluid column) *also* steady in time (locally conserved) and is diagnosable by inverting the sensitivity to balanced height given above. It is seen that $\hat{\eta}_b$ is, in fact, the sensitivity to balanced height as it appears in the adjoint of the statement of invertibility [(3)] that relates $\hat{\eta}_b$ to q'. The nature of the elliptic operator relating $\hat{q}$ to $\hat{\eta}_b$ implies that $\hat{q}$ will be smoother and of larger scale than $\hat{\eta}_b$—just as the sensitivity to barotropic vorticity is of larger scale than the sensitivity to streamfunction (Kleist and Morgan 2005a).

c. *Diagnostics*

Below we develop diagnostics for sensitivities to other nonmodel variables, including streamfunction, velocity potential, and the components of the horizontal ageostrophic flow. To derive sensitivities to streamfunction (ψ) and velocity potential (χ), each component of the wind is Helmholtz partitioned into nondivergent and irrotational parts,

$$u' = -\frac{\partial\psi}{\partial y} + \frac{\partial\chi}{\partial x} \quad \text{and} \quad v' = \frac{\partial\psi}{\partial x}\frac{\partial\chi}{\partial y}.$$

The adjoint of this partitioning yields

$$\hat{\psi} = -\left(\frac{\partial\hat{v}}{\partial x} - \frac{\partial\hat{u}}{\partial y}\right) = \nabla^2\hat{\zeta} \quad \text{and} \quad \hat{\chi} = -\left(\frac{\partial\hat{u}}{\partial x} + \frac{\partial\hat{v}}{\partial y}\right) = \nabla^2\hat{\delta}$$

where the last equalities for sensitivity to vorticity and divergence follow from Kleist and Morgan (2005a). To calculate sensitivity to the imbalanced (ageostrophic) flow, we write the ageostrophic components of the flow as the difference between the full flow and the geostrophic flow:

$$u_{\text{ag}} = -\frac{\partial\psi}{\partial y} + \frac{\partial\chi}{\partial x} + \frac{g}{f}\frac{\partial\eta}{\partial y}, \quad v_{\text{ag}} = \frac{\partial\psi}{\partial x} + \frac{\partial\chi}{\partial y} - \frac{g}{f}\frac{\partial\eta}{\partial x}, \quad \text{and}$$
$$q' = \frac{1}{H}\nabla^2\psi - \frac{f\eta}{H^2}.$$

The adjoint of this partitioning, coupled with the definition of PV, provides expressions for the sensitivities to

[1] In the discussion to follow, variables with a "hat" are adjoint variables; that is, the gradient of a response function R with respect to a model state $\mathbf{x}$, $\partial R/\partial\mathbf{x}$, is written as $\hat{\mathbf{x}}$.

streamfunction ($\hat{\psi}$), velocity potential ($\hat{\chi}$), and a diagnostic for sensitivities to perturbation height:

$$\hat{\psi} = \frac{1}{H}\nabla^2\hat{q} - \left(\frac{\partial \hat{v}_{ag}}{\partial x} - \frac{\partial \hat{u}_{ag}}{\partial y}\right) = \nabla^2\hat{\zeta}, \tag{8a}$$

$$\hat{\chi} = -\left(\frac{\partial \hat{u}_{ag}}{\partial x} + \frac{\partial \hat{v}_{ag}}{\partial y}\right) = \nabla^2\hat{\delta}, \tag{8b}$$

$$\hat{\eta} = -\frac{f}{H^2}\hat{q} + \frac{g}{f}\left(\frac{\partial \hat{v}_{ag}}{\partial x} - \frac{\partial \hat{u}_{ag}}{\partial y}\right). \tag{8c}$$

We may combine (8b) with (8c) to derive diagnostics for the sensitivities to the ageostrophic components of the flow:

$$\nabla^2\hat{u}_{ag} = -\frac{f^2}{gH^2}\frac{\partial \hat{q}}{\partial y} - \frac{\partial \hat{\chi}}{\partial x} - \frac{f}{g}\frac{\partial \hat{\eta}}{\partial y} \tag{9a}$$

and

$$\nabla^2\hat{v}_{ag} = \frac{f^2}{gH^2}\frac{\partial \hat{q}}{\partial x} - \frac{\partial \hat{\chi}}{\partial y} + \frac{f}{g}\frac{\partial \hat{\eta}}{\partial x}. \tag{9b}$$

d. Long-term behavior of the adjoint system

The shallow water adjoint system [(4)] has a steady, nondivergent solution obtainable by setting the time tendencies in the system to zero: $\hat{u} = -(H/f)\partial\hat{\eta}/\partial y$ and $\hat{v} = (H/f)\partial\hat{\eta}/\partial x$. This solution is degenerate in the sense that any $\hat{\eta}$ would satisfy the condition of nondivergence. Following a period of adjustment, during which sensitivities to ageostrophic motions have propagated out of the region of the initial adjoint forcing, a unique, steady solution is determined from the sensitivity to PV, $\hat{q}$; from (8c) for $t \to -\infty$, $\hat{\eta} = -(f/H^2)\hat{q} + (g/f)(\partial\hat{v}_{ag}/\partial x - \partial\hat{u}_{ag}/\partial y) \cong -(f/H^2)\hat{q}$ as $\hat{u}_{ag}$ and $\hat{v}_{ag} \to 0$. Recall that $\hat{q}$ is the solution to (7) via the inversion of the sensitivity to balanced height, $\hat{\eta}$. In the near-field (in the vicinity of the adjoint forcing at $t = t_f$), the long-term behavior of the system in the near-field is therefore

$$\hat{\eta}_{t\to-\infty} = -\frac{f}{H^2}\hat{q}, \tag{10a}$$

$$\hat{u}_{t\to-\infty} = -\frac{H}{f}\frac{\partial \hat{\eta}_{t\to-\infty}}{\partial y} = \frac{1}{H}\frac{\partial \hat{q}}{\partial y}, \tag{10b}$$

$$\hat{v}_{t\to-\infty} = \frac{H}{f}\frac{\partial \hat{\eta}_{t\to-\infty}}{\partial x} = -\frac{1}{H}\frac{\partial \hat{q}}{\partial x}. \tag{10c}$$

Using (10b) and (10c), the sensitivities to the ageostrophic components of the flow for long "backward" integrations (i.e., as $t \to -\infty$) may be written as

$$\nabla^2\hat{u}_{ag} = \frac{1}{L_r^2}\left(-u_{t\to-\infty} + L_r^2\nabla^2\hat{u}_\chi - \frac{H}{f}\frac{\partial \eta_{t\to-\infty}}{\partial y}\right) \cong \nabla^2\hat{u}_\chi$$

and

$$\nabla^2\hat{v}_{ag} = \frac{1}{L_r^2}\left(-v_{t\to-\infty} + L_r^2\nabla^2\hat{v}_\chi + \frac{H}{f}\frac{\partial \hat{\eta}_{t\to-\infty}}{\partial x}\right) \cong \nabla^2\hat{v}_\chi.$$

This result suggests that, in the vicinity of the prescribed adjoint forcing, *where adjustment has taken place*, sensitivities to ageostrophic motions are equivalent to sensitivities to the irrotational flow.

A summary of these diagnostic results is found in Table 1.

3. Model setup and experiments

a. Description of model setup

Numerical experiments are used to test the analytical results of the prior section. The linearized shallow wave equations (SWEs) are discretized on a 64 000 km × 64 000 km periodic Arakawa C grid with a uniform grid spacing of $\Delta x = \Delta y = 100$ km (i.e., 640 × 640 grid points. Centered finite differencing of spatial derivatives is used. The model is numerically integrated using the leapfrog scheme after a forward Euler time step. The time step chosen for the model is $\Delta t = 120$ s. The model is on an f plane at 38.25°N. The depth of the system at rest is $H = 8485.4$ m. These parameters yield a deformation radius, $L_r = (gh)^{1/2}/f = 3194$ km. The model code is developed as a line-by-line transpose of the code for the linearized system and is independent of the analytical analysis presented in the prior section. The diagnostic calculations of sensitivities to nonmodel variables are coded directly from the analytical results of the prior section. All variables plotted are calculated at or interpolated to the η grid points. The results are presented on a much smaller 120 × 120 gridpoint domain (centered on the computational domain). There is no qualitative or quantitative impact of the periodic boundary conditions of the larger domain on the solutions presented in this subset of the computational domain for the period of integration chosen.

b. Experiments

To illustrate the implications of the analytical results, we will consider first the adjustment of sensitivities for three adjoint forcings: (i) the sensitivity to an unbalanced zonal wind averaged over a box; (ii) the sensitivity of a nondivergent wind; and (iii) the sensitivity of an unbalanced height. The first case is similar to that associated with the R_2 response function considered by Kleist and Morgan (2005a, their Fig. 17) within the MM5 adjoint modeling system. In the final two cases, the form of the initial perturbation is based on a Gaussian function like those used in the geostrophic adjustment study of Barwell and Bromley (1988). The adjoint forcing

TABLE 1. Comparison of the forward and adjoint shallow water systems (rows 1–6), including diagnostics (rows 7–9) for the sensitivities to streamfunction ($\hat{\psi}$) and velocity potential ($\hat{\chi}$); sensitivities to vorticity ($\hat{\zeta}$) and divergence ($\hat{\delta}$); sensitivities to PV ($\hat{q}$) and balanced height ($\hat{\eta}_b$); and sensitivity to the ageostrophic flow ($\hat{u}_{ag}, \hat{v}_{ag}$), and sensitivities to the "adjusted" flow. Results in rows 4–6, 8, and 9 for the adjoint system are entirely new.

		Forward system	Adjoint system
1	Zonal momentum	$\partial u'/\partial t = fv' - g\partial\eta/\partial x$	$-\partial\hat{u}/\partial t = -f\hat{v} + H(\partial\hat{\eta}/\partial x)$
2	Meridional momentum	$\partial v'/\partial t = -fu' - g\partial\eta/\partial y$	$-\partial\hat{v}/\partial t = +f\hat{u} + H(\partial\hat{\eta}/\partial y)$
3	Mass continuity	$\partial\eta/\partial t = -H(\partial u'/\partial x + \partial v'/\partial y)$	$-\partial\hat{\eta}/\partial t = g(\partial\hat{u}/\partial x + \partial\hat{v}/\partial y)$
4	Conserved variable	$q' = -(1/H)(\partial u'/\partial y) + (1/H)(\partial v'/\partial y) - f\eta H^2$	$\hat{\eta}_b = \hat{\eta} - (g/f)(\partial\hat{v}/\partial x - \partial\hat{u}/\partial y)$
5	Combined system	$\partial^2\eta/\partial t^2 - c^2\nabla^2\eta + f^2\eta = -fH^2q'(x, y, t = 0)$	$\partial^2\hat{\eta}/\partial t^2 - c^2\nabla^2\hat{\eta} + f^2\hat{\eta} = -f^2\hat{\eta}_b(x, y, t = t_f)$
6	Inversion	$\nabla^2\eta_b - (f^2/gH)\eta_b = (Hf/g)q'(x, y, t = 0)$	$\nabla^2\hat{q} - (f^2/gH)\hat{q} = (Hf/g)\hat{\eta}_b(x, y, t = t_f)$
7	Diagnostics (part 1)	$u' = -\partial\psi/\partial y + \partial\chi/\partial x$ $v' = \partial\psi/\partial y + \partial\chi/\partial y$	$\hat{\psi} = -(\partial\hat{v}/\partial x - \partial\hat{u}/\partial y) = \nabla^2\hat{\zeta}$ $\hat{\chi} = -(\partial\hat{u}/\partial x + \partial\hat{v}/\partial y) = \nabla^2\hat{\delta}$
8	Diagnostics (part 2)	$u_{ag} = -\partial\psi/\partial y + \partial\chi/\partial x + (g/f)\partial\eta/\partial y$ $v_{ag} = \partial\psi/\partial x + \partial\chi/\partial y - (g/f)\partial\eta/\partial x$	$\nabla^2\hat{u}_{ag} = -(f^2/gH^2)(\partial\hat{q}/\partial y) - (\partial\hat{\chi}/\partial x) - (f/g)(\partial\hat{\eta}/\partial y)$ $\nabla^2\hat{v}_{ag} = (f^2/gH^2)(\partial\hat{q}/\partial x) - (\partial\hat{\chi}/\partial y) + (f/g)(\partial\hat{\eta}/\partial x)$
9	Adjusted flow	η_b from forward PV inversion (6) $u_b = -(g/f)\partial\eta_b/\partial y$ $v_b = (g/f)\partial\eta_b/\partial x$	$\hat{\eta}_{t\to-\infty} = -(f/H^2)\hat{q}$ $\hat{u}_{t\to-\infty} = -(H/f)\partial\hat{\eta}_{t\to-\infty}/\partial y = (1/H)\partial\hat{q}/\partial y$ $\partial\hat{v}_{t\to-\infty} = (H/f)\partial\hat{\eta}_{t\to-\infty}/\partial x = -(1/H)\partial\hat{q}/\partial x$

(i.e., the adjoint state used to initialize the adjoint model) for each of the three cases are shown in Fig. 1. In addition, the sensitivities to the balanced height, $\hat{\eta}_b$, are also shown. For the last two experiments, we specify the final time adjoint state without reference to the specific response functions from which they were derived.

1) ADJUSTMENT OF AN UNBALANCED SENSITIVITY OF ZONAL WIND IN A BOX

The adjoint state used to initialize the adjoint model at $t = t_f$ (i.e., the adjoint "forcing") for this experiment is given by

$$\hat{u}(305 \le i \le 335, 305 \le j \le 335, t = t_f) = 10,$$
$$\hat{v}(i, j, t = t_f) = 0, \quad \hat{\eta}(i, j, t = t_f) = 0.^2$$

This adjoint initial condition is proportional to that associated with the sensitivity of the average zonal flow in a box of 31 grid points (3100 km) on a side centered in the middle of the model domain. At each grid point, the sensitivity to the zonal flow is a specified constant (Fig. 1a), with no sensitivities to the meridional component of the flow $\hat{v}$ or to the height field $\hat{\eta}$. The sensitivities to wind (Fig. 1a) are displayed as sensitivity vectors (Kleist and Morgan 2005a).[3] For this case then, the sensitivity to balanced height is entirely associated with the curl of the sensitivity to wind and is confined to the northern and southern boundaries of the box.

The evolution of the sensitivities to the flow and height are shown in Figs. 2a,c,e. Instantaneous sensitivities to height are shown as fill patterns and sensitivity to wind as vectors. The long-term (i.e., for $t \to -\infty$) sensitivity to height as predicted by the distribution of the sensitivity to PV, $\hat{\eta} \cong -(f/H^2)\hat{q}$, is shown as contours. Figure 2a is of the adjoint forcing for this experiment (repeated from Fig. 1a) along with the sensitivity to the long-term height field. Note that this sensitivity to long-term height, which is proportional to the sensitivity to PV, is much broader than the sensitivity to balanced height—a result of the inversion in (7).

Two hours into the backward integration (Fig. 2c), a robust sensitivity to height has developed. This sensitivity is consistent with a southwest-to-northeast dipole of positive to negative height perturbations placed in the system to instantaneously "slosh" fluid to the northeast. This northeastward-directed flow would then be torqued clockwise by the Coriolis force to create a zonal flow 2 h later. The sensitivity vectors (for the sensitivity to wind) indicate a northeastward-directed flow that would be similarly torqued.

Six hours back into the integration (Fig. 2e), a north-to-south dipole emerges in the sensitivity to height near the region of the initial imbalance, while farther out from the location of the forcing, evidence for shallow water gravity wave–like features appear. The maximum in the amplitude of the sensitivity to height are collocated with the sensitivity to balanced height (Fig. 1a) but are of larger scale as anticipated from (7). The sensitivity to the horizontal flow is characterized by a dipole in the curl of the sensitivities to the horizontal wind components, with a cyclonic curl to the north and an anticyclonic curl to the south.

Figures 2b,d,f show the evolution of the sensitivity to the divergent flow and the sensitivity to divergence ($\hat{\delta}$) at the initial time, 2 h back, and 6 h back. At $t = t_f$ (Fig. 2b), the sensitivity to divergence is oriented in an east-to-west dipole straddling the box in which the

[2] The indices i and j represent the gridpoint numbers in the zonal and meridional directions, respectively.

[3] For clarity, only every third vector is plotted.

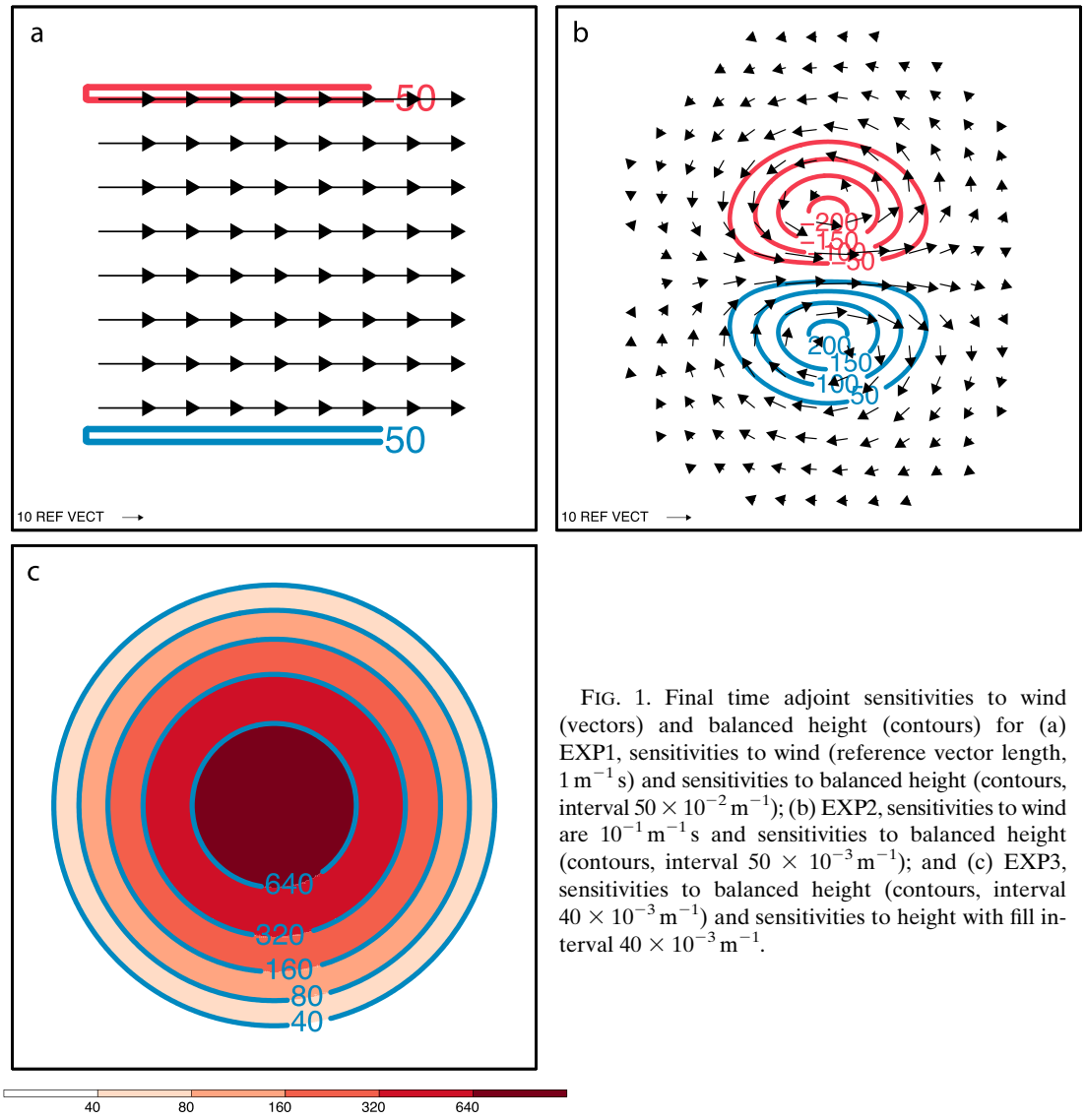

FIG. 1. Final time adjoint sensitivities to wind (vectors) and balanced height (contours) for (a) EXP1, sensitivities to wind (reference vector length, $1\,m^{-1}\,s$) and sensitivities to balanced height (contours, interval $50 \times 10^{-2}\,m^{-1}$); (b) EXP2, sensitivities to wind are $10^{-1}\,m^{-1}\,s$ and sensitivities to balanced height (contours, interval $50 \times 10^{-3}\,m^{-1}$); and (c) EXP3, sensitivities to balanced height (contours, interval $40 \times 10^{-3}\,m^{-1}$) and sensitivities to height with fill interval $40 \times 10^{-3}\,m^{-1}$.

adjoint forcing for this experiment was constructed. At $t = t_f - 2$ h, the amplitude of $\hat{\delta}$ has significantly decreased and the dipole has rotated counterclockwise. By $t = t_f - 6$ h, the distribution of $\hat{\delta}$ is characterized by two crescents farther removed from the location of the initial forcing. The maxima of the crescent-shaped $\hat{\delta}$ distribution are positively correlated with $\hat{\eta}$. The sensitivities to the divergent wind are maximized initially in the vicinity (both upstream and downstream) of the adjoint forcing (Fig. 2b), but 6 h later they have all but vanished at the site of the initial forcing while maintaining amplitude in the vicinity of the maxima in the crescent pattern of $\hat{\delta}$ described earlier.

2) ADJUSTMENT OF AN UNBALANCED SENSITIVITY OF NONDIVERGENT WIND

The adjoint state used to initialize the adjoint model for experiment 2 (EXP 2) is

$$\hat{u}(r,\theta,t=t_f) = U\left(1 - \frac{r^2}{d^2}\sin\theta\right)\exp\left(\frac{-r^2}{2d^2}\right),$$

$$\hat{v}(r,\theta,t=t_f) = \frac{Ur^2}{2d^2}\sin 2\theta \exp\left(\frac{-r^2}{2d^2}\right), \quad \hat{\eta}(r,\theta,t=t_f) = 0.$$

This initial condition for this experiment is shown in Fig. 1c (and in Fig. 4a). As with EXP1, the sensitivity to balanced height is entirely determined by the curl of the sensitivity to wind; however, in this case (as was the case for EXP2) the smoothness of the initial forcing results in a smooth north-to-south dipole of $\hat{\eta}_b$ (Fig. 3a).

The evolution of the sensitivities to the flow and height are shown in Figs. 3a,c,e. As the adjoint integration proceeds backward in time, a dipole pattern of sensitivities to height develops within just 2 h (Fig. 3c). This rapid development of a sensitivity to

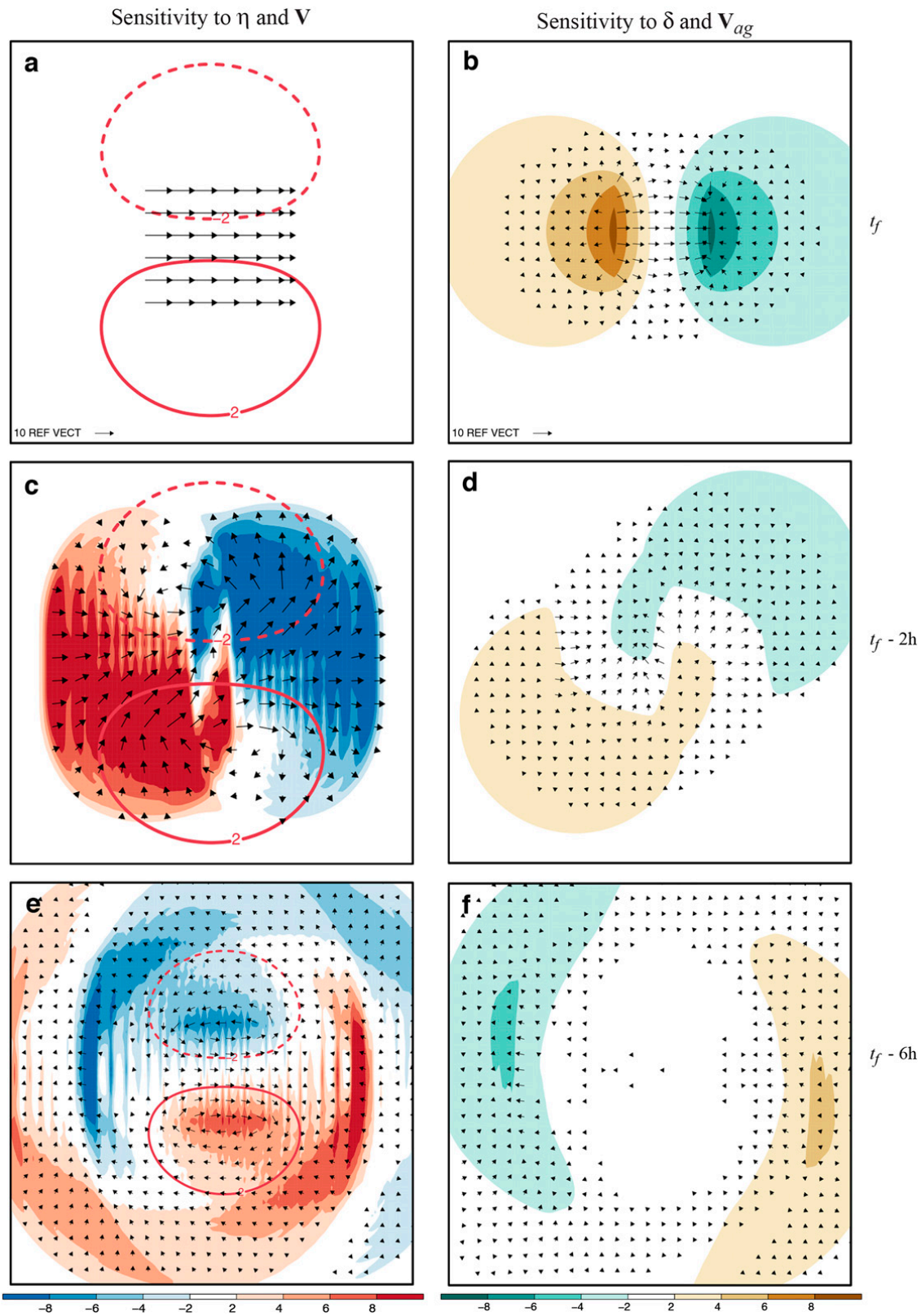

FIG. 2. For experiment EXP1 (a) sensitivity to wind, sensitivity to height (color fill, interval $2 \times 10^{-3}\,\mathrm{m}^{-1}$), and sensitivity to height for $t \to -\infty$ as diagnosed from (10b) and (10c) (contours, interval $2 \times 10^{-3}\,\mathrm{m}^{-1}$) at $t = t_f$; (b) sensitivity to divergence (color fill, interval 2×10^{-5} s) and sensitivity to the irrotational wind, at $t = 24$ h; (c) as in (a), but for $t = t_f - 2$ h; (d) as in (b), but for $t = t_f - 2$ h; (e) as in (a), but for $t = t_f - 6$h; and (f) as in (b), but for $t = t_f - 6$ h.

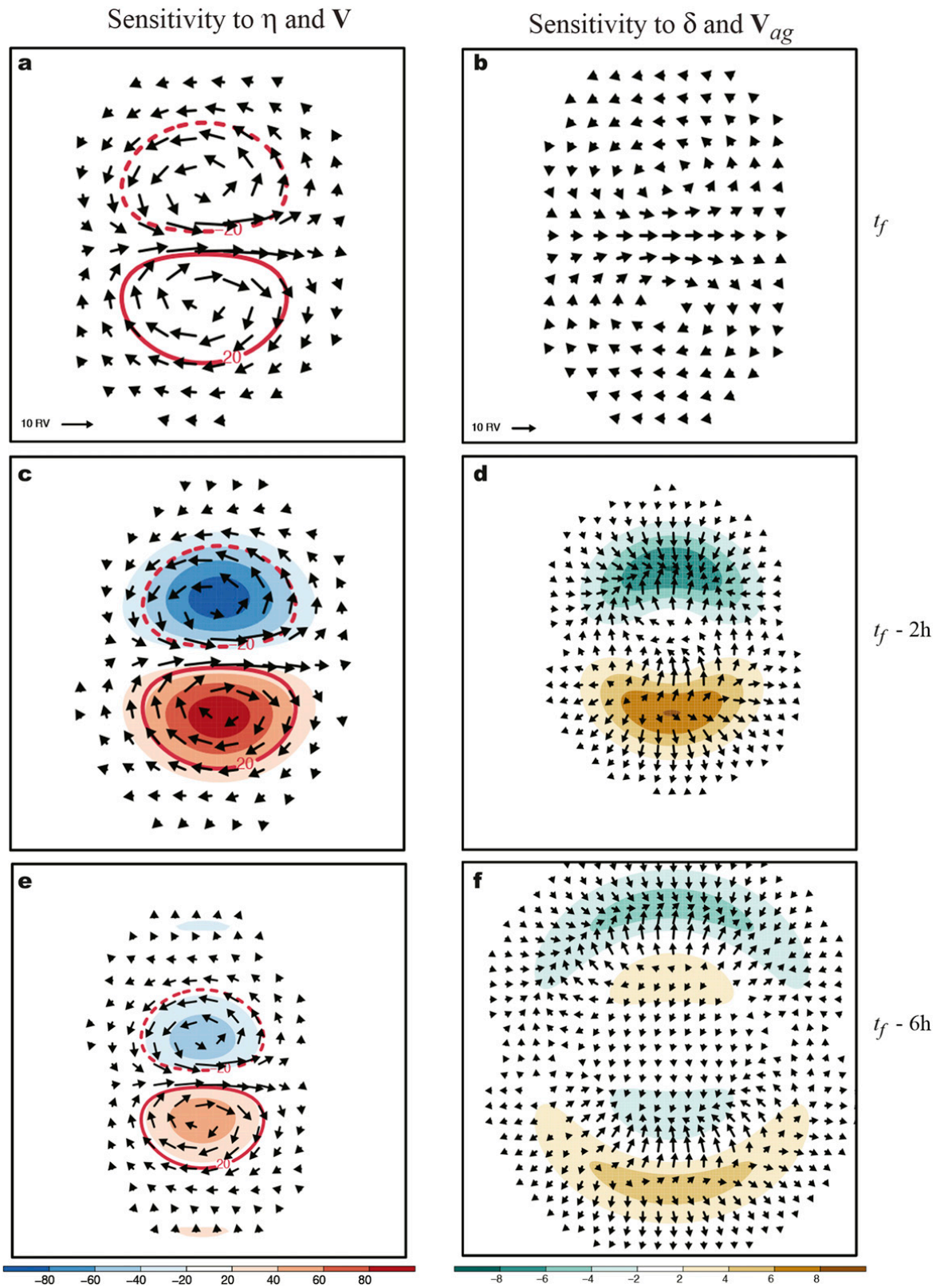

FIG. 3. For experiment EXP2 (a) sensitivity to wind, sensitivity to height (color fill, interval $20 \times 10^{-3}\,\mathrm{m}^{-1}$), and sensitivity to height for $t \to -\infty$ as diagnosed from (10b) and (10c) (contours, interval $20 \times 10^{-3}\,\mathrm{m}^{-1}$) at $t = t_f$; (b) sensitivity to divergence (color fill, interval $2 \times 10^{-5}\,\mathrm{s}$) and sensitivity to the ageostrophic wind, at $t = 24$ h; (c) as in (a), but for $t = t_f - 2$ h; (d) as in (b), but for $t = t_f - 2$ h; (e) as in (a), but for $t = t_f - 4$ h; and (f) as in (b), but for $t = t_f - 4$ h.

height can be seen as consistent with the sensitivities to the ageostrophic wind and sensitivity to divergence supporting a dipole pattern of sensitivities to divergence (convergence) and divergent (convergent) ageostrophic flow of fluid to the south (north). By $t = t_f - 6$ h (Figs. 3e,f), while the dipole pattern persists, the sensitivities to height have diminished from their earlier values, and a gravity wave–like structure in the sensitivity to height propagating northward and southward from the location of the prescribe adjoint forcing is evident. Further, the sensitivities to the wind and divergence (Fig. 3f) support this interpretation.

3) Adjustment of an unbalanced sensitivity of height

The adjoint state used to initialize the adjoint model for EXP3 is given by

$$\hat{\eta}(r,\theta,t=0) = h_0 \exp\left(\frac{-r^2}{2d^2}\right),$$
$$\hat{u}(r,\theta,t=0) = \hat{v}(r,\theta,t=0) = 0 \quad \text{with} \quad h_0 = 10.$$

The initial condition for this experiment is shown in Figs. 1d, 4a. In contrast to the prior experiments, in this experiment because the sensitivity to the flow field is zero, the sensitivity to the conserved dynamical variable in the adjoint model, balanced height, is determined by the sensitivity to the height field (Fig. 5a), and therefore $\hat{\eta}_b = \hat{\eta}$ (Fig. 4a). The sensitivity to the ageostrophic wind is purely nondivergent and cyclonic (Fig. 4b).

Two hours into the (backward) integration of the adjoint model (Fig. 4c), the initial maximum in the sensitivity to height has collapsed to a minimum and spread out radially from its initial location with a gravity wave–like structure (Barwell and Bromley 1988). The sensitivity to wind is largely convergent with an anticyclonic curl (Fig. 4c). Consistent with this description, the sensitivity to divergence is negative with the sensitivity to the ageostrophic wind dominated by a convergent, nearly irrotational component (Fig. 4d). Four hours later, near the location of the initial forcing, the sensitivity to height has returned to positive, with the flow predominantly anticyclonic and weakly divergent (Figs. 4e,f). Farther out from the location of the initial forcing, the gravity wave–like structure is evident in alternating rings of positive and negative sensitivity to height and a ring of negative sensitivity to divergence. The distribution of sensitivity to the ageostrophic wind is nearly zero in the location of the initial forcing, while farther out it is of large amplitude and consistent with convergence into the region of negative sensitivity to divergence (Fig. 4f).

The initial distribution of sensitivities to ageostrophic flow (Fig. 4b) may be understood by combining (8c) and (10a) to form $\partial\hat{v}_{ag}/\partial x - \partial\hat{u}_{ag}/\partial y = (f/g)(\hat{\eta} - \hat{\eta}_{t\to-\infty})$. As noted above, the final time sensitivity to height is more spread out and of far less amplitude than its initial value. As a consequence, $\hat{\eta} - \hat{\eta}_{t\to-\infty} > 0$, implying that the sensitivity to the *ageostrophic* flow field is cyclonic.

4) Resulting adjoint state following long-term adjoint integration

By 24 h of adjoint integration, there is no longer evidence of the gravity wave–like structures in the subdomains shown, as those structures have now propagated out of view, away from the initial adjoint forcing. The sensitivities to the ageostrophic wind and to divergence are both zero within the domain (not shown). The long-term numerical solutions to the adjoint shallow water system agree with the anticipated results derived analytically. Specifically, the resulting long-term integration (24 h back) produces a steady-state distribution of sensitivities to height that are exactly equal to the expected distribution given by (10a) [$\hat{\eta} \cong -(f/H^2)\hat{q}$] while the long-term sensitivities to wind, $\hat{\mathbf{V}}_{t\to-\infty}$, are given by $\hat{\mathbf{V}}_{t\to-\infty} = (H/f)\hat{\mathbf{k}} \times \nabla\hat{\eta}_{t\to-\infty}$. It is this long-term state that we term the *adjusted adjoint state*. That this adjusted adjoint state is determined by the sensitivity to PV$\hat{q}$ implies that $\hat{q}$, and that as a consequence of (7), the sensitivity to balanced height $\hat{\eta}_b$ are indeed conserved.

Experiment EXP4 provides an excellent example of the conservation of the sensitivity to balanced height. For EXP4, at the adjoint initialization time, $t = t_f$, because $\hat{u} = \hat{v} = 0$, the sensitivity to height and the sensitivity to balanced height are equivalent [see (5)]. As seen in Figs. 4a,c,e, 5c, as the adjoint fields evolve (backward in time), sensitivities to height become smaller so that $\hat{\eta}_t < \hat{\eta}_{t_f}$ for $t < t_f$. Conservation of $\hat{\eta}_b$ requires that the curl of the sensitivity to wind becomes anticyclonic during the integration of the adjoint model so that $\hat{\eta}_b = \hat{\eta} - (g/f)(\partial\hat{v}/\partial x - \partial\hat{u}/\partial y)$ is constant. The two prior experiments in which the adjoint state is initialized with the sensitivities to wind alone also reveal evidence of this conservation. For those experiments, the dipoles (negative to the north, positive to the south) in the adjusted adjoint state (Figs. 5a,b) are centered precisely in the locations where dipoles in the vertical component of the curl of the initialized adjoint state sensitivity to wind exist (cyclonic to the north, anticyclonic to the south). The decrease in the absolute value of the curl of the wind sensitivity requires, via conservation of balanced height, a corresponding change in the sensitivity to height.

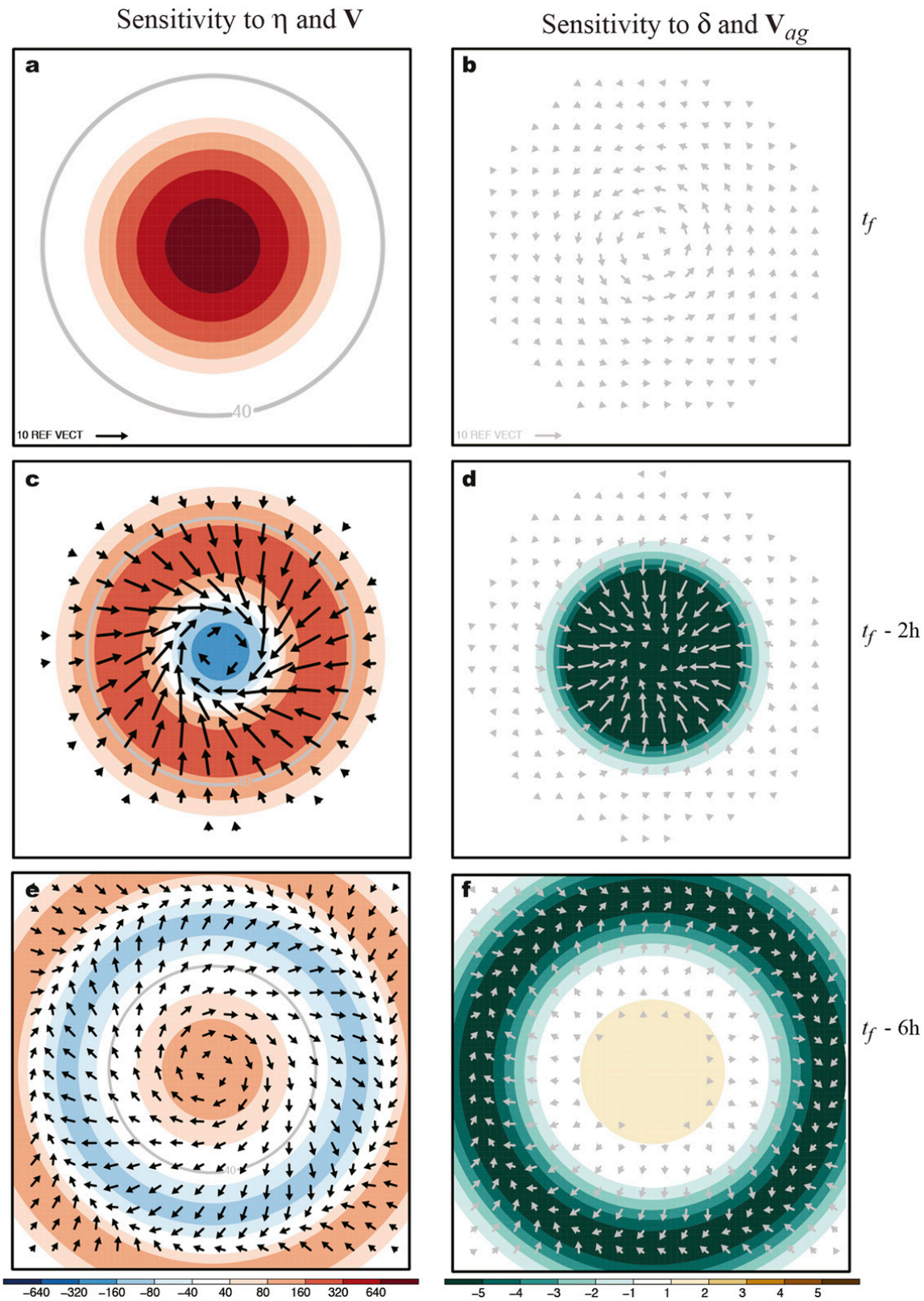

FIG. 4. For experiment EXP3 (a) sensitivity to wind, sensitivity to height (color fill, interval 40×10^{-2}, 80×10^{-2}, 160×10^{-2}, 320×10^{-2} m^{-1}), and sensitivity to height for $t \to -\infty$ as diagnosed from (10b) and (10c) (contours, interval 40×10^{-2} m^{-1}) at $t = t_f$; (b) sensitivity to divergence (color fill, interval 1×10^{7} m^{-1} s) and sensitivity to the ageostrophic wind (reference vector length, 1×10^{1} m^{-1} s), at $t = 24$ h; (c) as in (a), but for $t = t_f - 2$ h; (d) as in (b), but for $t = t_f - 2$ h; (e) as in (a), but for $t = t_f - 6$ h; and (f) as in (b), but for $t = t_f - 6$ h.

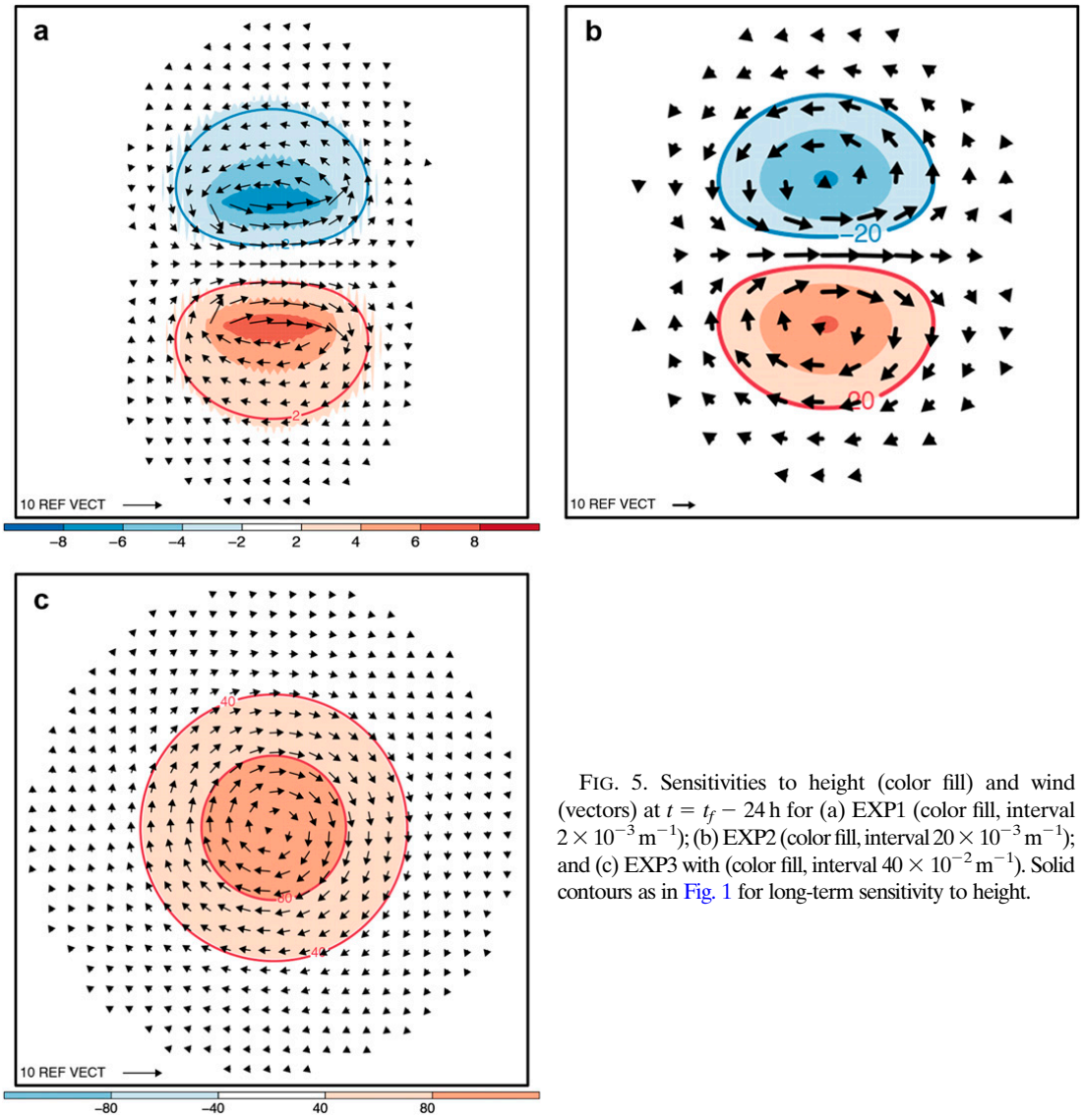

FIG. 5. Sensitivities to height (color fill) and wind (vectors) at $t = t_f - 24$ h for (a) EXP1 (color fill, interval $2 \times 10^{-3}\,\mathrm{m}^{-1}$); (b) EXP2 (color fill, interval $20 \times 10^{-3}\,\mathrm{m}^{-1}$); and (c) EXP3 with (color fill, interval $40 \times 10^{-2}\,\mathrm{m}^{-1}$). Solid contours as in Fig. 1 for long-term sensitivity to height.

4. Summary, discussion, significance, and future work

a. Summary

Analytic results and numerical experimentation have revealed that the dynamics of the adjoint SW system are similar to those of the forward SW system in that "backward" (forward) evolution of an adjoint (forward) model from an "unbalanced" final (initial) adjoint (forward) state is characterized by a radiation of gravity waves and emergence of a steady state. The earlier adjoint states are linked to the prescribed, final state (adjoint forcing) through the locally conserved dynamical variables of the shallow water system: the sensitivity to "balanced height" $\hat{\eta}_b$ and sensitivity to PV $\hat{q}$. The sensitivity to balanced height is determined from the adjoint sensitivity forcings for $\hat{u}$, $\hat{v}$, and $\hat{\eta}$ initialized at time $t = t_f$ using (5). The sensitivity to PV is diagnosed from an inversion of the distribution of $\hat{\eta}_b$ from (7). That the sensitivity to PV is conserved locally (i.e., is steady in time) is anticipated, as the PV of a fluid column in the forward shallow water system is conserved locally.

The sensitivity to PV determines the long-time ($t \to -\infty$), steady behavior of the adjoint model sensitivity to height, $\hat{\eta}_{t\to-\infty} = -(f/H^2)\hat{q}$ [(10a)]. In the vicinity of the initial adjoint forcing, the long-time, steady-state behavior of the adjoint system (linearized about a state at rest) is characterized by nondivergent flow resembling geostrophic balance, with sensitivities to the wind components proportional the gradients of the sensitivity to PV: $\hat{u}_{t\to-\infty} = (1/H)\partial\hat{q}/\partial y$ [(10b)] and $\hat{v}_{t\to-\infty} = (1/H)\partial\hat{q}/\partial x$ [(10c)]. The process by which this long-time adjoint state emerges during the backward-in-time adjoint integration is termed *adjoint adjustment*.

During adjoint adjustment, in the single layer, *f*-plane shallow system gravity wave–like structures in the adjoint sensitivity fields radiate away from the region of the specified adjoint forcing. As a consequence, at the location of the adjoint forcing, there is no "memory" of any initial imbalance (part of forcing that would project onto the gravity wave–like structures). These structures are characterized by sensitivities to the ageostrophic flow and divergence. For the portions of the flow that have achieved balance (i.e., where the adjustment has completed), sensitivities to both the ageostrophic and the irrotational flows are zero.

b. Discussion

1) Why focus on prescribed (i.e., $t = t_f$) unbalanced sensitivities?

Unbalanced sensitivities (as defined in this paper) do not describe sensitivities to unbalanced flow components, but rather they describe adjoint sensitivities that do not satisfy (10). The focus of the manuscript is on the backward-in-time evolution of the adjoint model solution from unbalanced adjoint forcings. Such forcings are, in fact, the most common type of sensitivity encountered in most extant adjoint studies. While a final time model state may be balanced (in the traditional sense), it is the gradient of a chosen response function with respect to that model state that is the adjoint forcing (adjoint input). In general, the choice of an arbitrary response function results in sensitivities that do not satisfy (10)—for example, a response function measuring the pressure at a point, areal-averaged vertical component of vorticity in a two- (or three-) dimensional domain, or, in a 4DVAR context, the gradient of the observational cost function. During the backward adjoint integration, the gradients of these response functions will radiate ultimately gravity wave–like structures from the region of the prescribed adjoint forcing (adjoint model initial condition). If one were to specify gradients of a response function that did satisfy (10), then the adjoint sensitivities $\hat{u}$, $\hat{v}$, and $\hat{\eta}$ would be steady.

2) Sensitivity to balanced height vs. "balanced" sensitivity to height

As described in this paper, within the context of the rotating shallow water system, a balanced adjoint state emerges after sufficiently long integration backward in time from an arbitrary distribution of sensitivities to height and horizontal velocity. The (balanced) long-term sensitivity to height $\hat{\eta}_{t\to-\infty}$ is distinguished from the conserved sensitivity to balanced height $\hat{\eta}_b$. The sensitivity to balanced height is the variable that carries with it, the memory of the adjoint forcing [(5)]. The two sensitivities are equivalent only if the long-term sensitivity to horizontal velocity field vanishes, which would imply no horizontal variation in the long-term sensitivity to height.

3) Interpretation of results

The preceding work has shown that whenever there is an adjustment process that leads to a "balanced state" in the forward equations, there will be a corresponding adjustment process in the backward adjoint equations. The adjoint sensitivities to unbalanced flow (divergent or ageostrophic) calculated for the various response functions *in this system* imply that unbalanced perturbations that locally influence the final time response function must be associated with locally decreasing sensitivities as the backward integration proceeds.

An anonymous reviewer has suggested the following thought experiment: Consider a dynamical system, the state ($\mathbf{x}$) of which is defined by two components, $\mathbf{x}_R$ and $\mathbf{x}_G$. The temporal evolution of the system is such that the component $\mathbf{x}_G$ acts only weakly on $\mathbf{x}_R$ and that in addition any solution tends over a time scale T to a balance $B(\mathbf{x}_R, \mathbf{x}_G) = 0$, which defines X_G as a function of $\mathbf{x}_R$ so that $\mathbf{x}_G$ can be said to be "slaved" to $\mathbf{x}_R$ (e.g., Warn et al. 1995). This is essentially what happens in rotating geophysical flows, with $\mathbf{x}_R$ and $\mathbf{x}_G$ being, respectively, the Rossby wave and gravity wave components of the flow. In the simple linear case considered in this paper, the balance condition is simply $\mathbf{x}_G = 0$ (geostrophic balance, no gravity waves).

Consider now a balanced state $(\mathbf{x}_R^b, \mathbf{x}_G^b)$ with balance condition $B(\mathbf{x}_R^b, \mathbf{x}_G^b) = 0$, at some diagnostic time t_f, and a perturbation to component $\mathbf{x}_G$ at some earlier time $t < t_f - T$. By the time the system evolves to t_f, adjustment to the balanced state will have taken place and nothing will remain of the perturbation imposed at t. Thus, the adjoint integration corresponding to any response function R defined on the balanced state (X_b, G_b) *must* lead at any $t < t_f - T$ to the sensitivity with respect to $\mathbf{x}_G$, $\hat{\mathbf{x}}_G$, that is, equal to 0. For some response functions (e.g., $R = \mathbf{x}_R$), the sensitivity to $\mathbf{x}_G$ will be zero from the start of the adjoint integration at time t_f. For other response functions (such as $R = \mathbf{x}_G$), the sensitivity will tend to 0 through an adjustment process —the adjoint of the direct adjustment process. Fundamentally that is what has been observed in this study, and what Errico and Vukićević (1992) observed in their study. Indeed, the results presented in this manuscript are consistent with, and provide an explanation for, the interpretation of the results of Errico and Vukićević (1992), wherein short-term MM4 adjoint model adjoint sensitivities were dominated by response function sensitivity (to the horizontal velocity) structures describing the impact of external gravity wave velocity perturbations, while longer-term integrations yield

velocity and height sensitivities describing the impact of geostrophic perturbations (in the shallow water context, these are precisely the geostrophic perturbations noted in the preceding section. In short, what has been presented in this paper is a particular case of a much more general fact: *whenever an adjustment process results in the forward integration in the "slaving" of some component* $\mathbf{x}_G$ *to other components, then there must be a process in the adjoint integration leading to a damping of the sensitivity with respect to* $\mathbf{x}_G$.

That the sensitivity to PV determines the long-term backward sensitivity distribution for this system means that once $\hat{q}$ is evaluated, the long-term distributions of $\hat{u}$, $\hat{v}$, and $\hat{\eta}$ are determined. This allows a convenient single scaling of the perturbation horizontal velocity distribution, consistent with the perturbation height. Recalling the algebraic "swapping of variables," g and H, when compared with the forward system mentioned in section 2, one could readily determine (for any time, $t < t_f$) the geostrophically balanced wind and height perturbations needed to change the response function at the final time, $t = t_f$.

c. Significance

The results of the present study would imply that that there exists a quasi-conserved dynamical variable in (at the very least) hydrostatic models that determines to what adjoint state the sensitivities would adjust. It is possible that this variable is (closely related to) the sensitivity to (Ertel) potential vorticity. Arbogast (1998) demonstrates a variational minimization procedure for calculating the sensitivity to Ertel PV and sensitivities to the unbalanced horizontal flow from sensitivities to temperature and horizontal velocity. A similar procedure, applied to the adjoint f-plane shallow water system of the present study, would produce the same results shown in Table 1.

Kleist and Morgan (2005a) provide evidence that for nearly adiabatic forecast trajectory evolution, adjoint-derived sensitivities appear to follow isentropic surfaces. The results of the current study, coupled with the Kleist and Morgan (2005a) result, suggest an additional characteristic of the sensitivity to PV—that for an adiabatic and inviscid forecast trajectory, the sensitivity to Ertel PV would be *nearly conserved* following the (time-evolving) flow described by the NWP model basic-state forecast trajectory. The choice of "nearly conserved" versus "conserved" arises because the adjustment process in time-dependent nonlinear flows (Kuo and Polvani 2000) has been demonstrated to lead to irreversible deformation of PV attributed to the gravity waves generated during the adjustment process. If the PV were not conserved in the forecast trajectory, then it is doubtful the sensitivity to PV would be conserved during the backward integration. As a consequence, unlike the sensitivity to PV in a shallow water system linearized about a basic state at rest, however, it is anticipated that the distribution of sensitivity to PV would be susceptible also to deformation by the time-evolving, basic-state flow. The conservation and invertibility of the sensitivity to balanced height and the relationship between the sensitivity of balanced height and sensitivity to PV make these sensitivities valuable in identifying the salient features contained in sensitivities to the model state variables for quasi-balanced weather systems.

Knowledge of the nonconservation of PV (in particular, PV redistribution) coupled with sensitivities to PV would also be useful in synoptic case studies. Because "physical processes that produce large tendencies in regions of strong adjoint sensitivity are significant to the feature ... represented by the [response function]" (Langland et al. 1995, p. 1369), the key to interpretation of an adjoint sensitivity of a response function with respect to some function of the model state $f(\mathbf{x})$, $\partial R/\partial f(x)$ is the coincidence of the adjoint sensitivity field, with the Lagrangian tendency in that function $Df(x)/Dt$. If there are observed tendencies in PV that coincide with sensitivities to PV, one would be able to attribute significance to the processes (e.g., diabatic heating and friction) producing that PV tendency on changes in the response function measuring some aspect of the forecast.

With respect to 4DVAR data assimilation, the results from this study suggest that for an isolated observation (or collection of nearby observations at the same time), the portion of the gradient of the measure of the misfit of that observation from an NWP model background trajectory (assuming adiabatic and inviscid flow) that exists after the adjoint model is used to integrate that gradient back to the analysis time is that portion of the gradient that projects onto the sensitivity of the misfit to the potential vorticity at the observation time. Moreover, for sufficiently long time scales, the sensitivities of that misfit to the wind and temperature will be related to each other in a thermal-wind-type balance, with each diagnosable from the sensitivity to PV. Conversely, the results suggest that misrepresentation of PV conservation in the forward NWP model forecast trajectory can lead to errors in the misfit gradient at the initial time, thereby contributing to errors in the analysis.

d. Future work

The author proposes calculating the sensitivity to PV and unbalanced flow components in the Weather Research and Forecasting (WRF) Model adjoint (Zhang et al. 2013) using the framework proposed by Arbogast (1998)

and implemented by Decker (2010). In parallel, the author is calculating estimates of these very same sensitivities using ensemble-derived forecast sensitivities following the work of Ancell and Hakim (2007). These two approaches will diagnose previously uncalculated sensitivities to balanced and unbalanced components of the model state (e.g., sensitivities to the ageostrophic and divergent components of the flow). The author will evaluate the evolution of the sensitivity to variables, including PV and the ageostrophic and divergent wind components using the WRF adjoint system. These results will be compared with those of the shallow water adjoint system. The relationship between the ensemble and adjoint-derived forecast sensitivities—particularly the convergence of the two fields as the ensemble size is increased—will be assessed as well.

Acknowledgments. The author acknowledges gratefully the insightful and helpful comments and suggestions of three anonymous reviewers that greatly enhanced this manuscript. This work was supported by National Science Foundation Award AGS-1638194.

APPENDIX

Derivation of the Adjoint of the Shallow Water System

Mathematically, the *adjoint* of a linear operator $\mathbf{A}$ is an operator $\mathbf{A}^*$ that satisfies the relation $\langle \mathbf{x}, \mathbf{Ay}\rangle_m = \langle \mathbf{A}^*\mathbf{x}, \mathbf{y}\rangle_n$, where $\mathbf{x}$ and $\mathbf{y}$ are vectors (or functions) in R^m and R^n, which denote the vector space of m- and n-dimensional real vectors, respectively; and $\langle\ ,\ \rangle_m$ and $\langle\ ,\ \rangle_n$, which denote inner products in R^m and R^n, respectively. This definition of an adjoint operator, coupled with the notion that the adjoint of a linear operator is the transpose, $(\cdot)^{\mathrm{T}}$, of the matrix representation of that operator, provides a powerful, practical means of analytically and numerically generating adjoints for continuous and discrete operators. For linear operators on continuous functions, $f(x)$ and $g(x)$, the definition also applies. The adjoint of the derivative operator, d/dx, may be obtained using this definition of an adjoint along with the integration by parts to evaluate the inner product:

$$\left\langle f, \frac{d}{dx} g \right\rangle = \int_a^b f \frac{d}{dx} g \, dx = f(b)g(b) - f(a)g(a) - \int_a^b g \frac{d}{dx} f \, dx.$$

Assuming "natural" boundary conditions: $f(b)g(b) = f(a)g(a)$ results in

$$\left\langle f, \frac{d}{dx} g \right\rangle = -\int_a^b g \frac{d}{dx} f \, dx = -\int_a^b \left(-\frac{d}{dx} f\right) g \, dx = \left\langle -\frac{d}{dx} f, g \right\rangle.$$

Thus, the adjoint of d/dx is $-d/dx$.

Two time-varying linear systems of the form $\dot{\mathbf{x}} = \mathbf{Ax}$ and $-\dot{\hat{\mathbf{x}}} = \mathbf{A}^{\mathrm{T}}\hat{\mathbf{x}}$ are called *adjoint* to each other. The solution to the forward system ($\mathbf{x}$) and the solution to the adjoint system ($\hat{\mathbf{x}}$) are linked by the property that their inner product $\langle \hat{\mathbf{x}}, \mathbf{x}\rangle$ remains constant:

$$\frac{d}{dt}\langle \hat{\mathbf{x}}, \mathbf{x}\rangle = \langle \dot{\hat{\mathbf{x}}}, \hat{\mathbf{x}}\rangle + \langle \hat{\mathbf{x}}, \dot{\mathbf{x}}\rangle = \langle -\mathbf{A}^{\mathrm{T}}\hat{\mathbf{x}}, \mathbf{x}\rangle + \langle \hat{\mathbf{x}}, \mathbf{Ax}\rangle = (-\mathbf{A}^{\mathrm{T}}\hat{\mathbf{x}})^{\mathrm{T}}\mathbf{x} + \hat{\mathbf{x}}\mathbf{Ax} = 0.$$

The linearized shallow water system [(1)] may be written as

$$\begin{pmatrix} \dot{u} \\ \dot{v} \\ \dot{\eta} \end{pmatrix} = \begin{pmatrix} 0 & f & -g\dfrac{\partial}{\partial x} \\ -f & 0 & -g\dfrac{\partial}{\partial y} \\ -H\dfrac{\partial}{\partial x} & -H\dfrac{\partial}{\partial y} & 0 \end{pmatrix} \begin{pmatrix} u \\ v \\ \eta \end{pmatrix}.$$

The corresponding adjoint of the shallow water system [(4)] is then given by

$$-\begin{pmatrix} \dot{\hat{u}} \\ \dot{\hat{v}} \\ \dot{\hat{\eta}} \end{pmatrix} = \begin{pmatrix} 0 & -f & H\dfrac{\partial}{\partial x} \\ f & 0 & H\dfrac{\partial}{\partial y} \\ g\dfrac{\partial}{\partial x} & g\dfrac{\partial}{\partial y} & 0 \end{pmatrix} \begin{pmatrix} \hat{u} \\ \hat{v} \\ \hat{\eta} \end{pmatrix}.$$

REFERENCES

Ancell, B., and G. J. Hakim, 2007: Comparing adjoint- and ensemble-sensitivity analysis with applications to observation targeting. *Mon. Wea. Rev.*, **135**, 4117–4134, https://doi.org/10.1175/2007MWR1904.1.

Arbogast, P., 1998: Sensitivity to potential vorticity. *Quart. J. Roy. Meteor. Soc.*, **124**, 1605–1615, https://doi.org/10.1002/qj.49712454912.

Barwell, B. R., and R. A. Bromley, 1988: The adjustment of numerical weather prediction models to local perturbations. *Quart. J. Roy. Meteor. Soc.*, **114**, 665–689, https://doi.org/10.1002/qj.49711448107.

Buizza, R., J. Tribbia, F. Molteni, and T. Palmer, 1993: Computation of optimal unstable structures for a numerical weather

prediction model. *Tellus*, **45A**, 388–407, https://doi.org/10.3402/tellusa.v45i5.14901.

Decker, S. G., 2010: Nonlinear balance in terrain-following coordinates. *Mon. Wea. Rev.*, **138**, 605–624, https://doi.org/10.1175/2009MWR2971.1.

Doyle, J., C. Amerault, C. Reynolds, and P. A. Reinecke, 2014: Initial condition sensitivity and predictability of a severe extratropical cyclone using a moist adjoint. *Mon. Wea. Rev.*, **142**, 320–342, https://doi.org/10.1175/MWR-D-13-00201.1.

Errico, R. M., 1989: Theory and application of nonlinear normal mode initialization. NCAR Tech. Note NCAR/TN-344+IA, 144 pp. [Available from NCAR, P.O. Box 3000, Boulder, CO 80307-3000.]

——, and T. Vukićević, 1992: Sensitivity analysis using an adjoint of the PSU–NCAR mesoscale model. *Mon. Wea. Rev.*, **120**, 1644–1660, https://doi.org/10.1175/1520-0493(1992)120<1644:SAUAAO>2.0.CO;2.

Farrell, B. F., 1989: Optimal excitation of baroclinic waves. *J. Atmos. Sci.*, **46**, 1193–1206, https://doi.org/10.1175/1520-0469(1989)046<1193:OEOBW>2.0.CO;2.

Hall, M. C. G., D. G. Cacuci, and M. E. Schlesinger, 1982: Sensitivity analysis of a radiative convective model by the adjoint method. *J. Atmos. Sci.*, **39**, 2038–2050, https://doi.org/10.1175/1520-0469(1982)039<2038:SAOARC>2.0.CO;2.

Hoover, B. T., 2015: Identifying a barotropic growth mechanism in east Pacific tropical cyclogenesis using adjoint-derived sensitivity gradients. *J. Atmos. Sci.*, **72**, 1215–1234, https://doi.org/10.1175/JAS-D-14-0053.1.

——, and M. C. Morgan, 2011: Dynamical sensitivity analysis of tropical cyclone steering using an adjoint model. *Mon. Wea. Rev.*, **139**, 2761–2775, https://doi.org/10.1175/MWR-D-10-05084.1.

Keller, L. M., M. C. Morgan, D. D. Houghton, and R. A. Lazear, 2006: Synoptic–dynamic climatology of large-scale cyclones in the North Pacific. *Mon. Wea. Rev.*, **134**, 3567–3587, https://doi.org/10.1175/MWR3260.1.

Kleist, D. T., and M. C. Morgan, 2005a: Interpretation of the structure and evolution of adjoint-derived forecast sensitivity gradients. *Mon. Wea. Rev.*, **133**, 466–484, https://doi.org/10.1175/MWR-2865.1.

——, and ——, 2005b: Application of adjoint-derived forecast sensitivities to the 24–25 January 2000 U.S. East Coast snowstorm. *Mon. Wea. Rev.*, **133**, 3148–3175, https://doi.org/10.1175/MWR3023.1.

Klinker, E., F. Rabier, and R. Gelaro, 1998: Estimation of key analysis errors using the adjoint technique. *Quart. J. Roy. Meteor. Soc.*, **124**, 1909–1933, https://doi.org/10.1002/qj.49712455007.

Kuo, A., and L. Polvani, 2000: Nonlinear geotrophic adjustment, cyclone/anticyclone asymmetry, and potential vorticity rearrangement. *Phys. Fluids*, **12**, 1087–1100, https://doi.org/10.1063/1.870363.

Langland, R., R. L. Elsberry, and R. M. Errico, 1995: Evaluation of physical processes in an idealized extratropical cyclone using adjoint sensitivity. *Quart. J. Roy. Meteor. Soc.*, **121**, 1349–1386, https://doi.org/10.1002/qj.49712152608.

——, M. A. Shapiro, and R. Gelaro, 2002: Initial condition sensitivity and error growth in forecasts of the 25 January 2000 East Coast snowstorm. *Mon. Wea. Rev.*, **130**, 957–974, https://doi.org/10.1175/1520-0493(2002)130<0957:ICSAEG>2.0.CO;2.

Rabier, R., F. Klinker, P. E. Courtier, and A. Hollingsworth, 1996: Sensitivity of forecast errors to initial conditions. *Quart. J. Roy. Meteor. Soc.*, **122**, 121–150, https://doi.org/10.1002/qj.49712252906.

Rossby, C.-G., 1938: On the mutual adjustment of pressure and velocity distributions in certain simple current systems, II. *J. Mar. Res.*, **1**, 239–263, https://doi.org/10.1357/002224038806440520.

Talagrand, O., and P. Courtier, 1987: Variational assimilation of meteorological observations with the adjoint vorticity equation. I: Theory. *Quart. J. Roy. Meteor. Soc.*, **113**, 1311–1328, https://doi.org/10.1002/qj.49711347812.

Vukićević, T., and K. Raeder, 1995: Use of an adjoint model for finding triggers for Alpine lee cyclogenesis. *Mon. Wea. Rev.*, **123**, 800–816, https://doi.org/10.1175/1520-0493(1995)123<0800:UOAAMF>2.0.CO;2.

Warn, T., O. Bokhove, T. G. Shepherd, and G. K. Vallis, 1995: Rossby number expansions, slaving principles, and balance dynamics. *Quart. J. Roy. Meteor. Soc.*, **121**, 723–739, https://doi.org/10.1002/qj.49712152313.

Washington, W. M., 1964: A note on the adjustment towards geostrophic equilibrium in a simple fluid system. *Tellus*, **16**, 530–534, https://doi.org/10.3402/tellusa.v16i4.8985.

Zhang, X., X.-Y. Huang, and N. Pan, 2013: Development of the upgraded tangent linear and adjoint of the Weather Research and Forecasting (WRF) model. *J. Atmos. Oceanic Technol.*, **30**, 1180–1188, https://doi.org/10.1175/JTECH-D-12-00213.1.